NAL phase in K-rich portions of the lower mantle

NAL phase in K-rich portions of the lower mantle

Chie Kato,[1] Kei Hirose,[1,2,3] Tetsuya Komabayashi,[1] Haruka Ozawa,[1,3] and Yasuo Ohishi[4]

Received 1 August 2013; revised 13 September 2013; accepted 13 September 2013; published 8 October 2013.

[1] The stability of the K-rich new aluminous (NAL) phase was examined on the join $Na_{1.00}Mg_{2.00}Al_{4.80}Si_{1.15}O_{12}$-$K_{1.00}Mg_{2.00}Al_{4.80}Si_{1.15}O_{12}$ (Na100-K100) up to 144 GPa by X-ray diffraction in a laser-heated diamond anvil cell. Single-phase K100 and Na50K50 NAL were formed up to the lower mantle conditions, and the NAL phase coexisted with the calcium ferrite–type (CF) phase at 120 GPa and 2300 K for the Na75K25 bulk composition. This is a striking contrast to the K-free (Na100) NAL that becomes unstable above 27 GPa at 1850 K, which suggests that potassium stabilizes NAL at significantly higher pressures. K-rich NAL may host potassium in the lower mantle that contains K_2O more than 0.09 wt %. In addition, the NAL phase likely formed owing to partial melting in the ultralow-velocity zone or because of a basal magma ocean. Future seismological observations may clarify whether NAL is a radiogenic heat source above the core-mantle boundary. **Citation:** Kato, C., K. Hirose, T. Komabayashi, H. Ozawa, and Y. Ohishi (2013), NAL phase in K-rich portions of the lower mantle, *Geophys. Res. Lett.*, *40*, 5085–5088, doi:10.1002/grl.50966.

1. Introduction

[2] Potassium is an important heat-producing element, but its host phases under deep lower mantle conditions remain poorly known [*Wang and Takahashi*, 2000; *Miyajima et al*., 2001; *Lee et al*., 2009]. The K_2O content of pyrolitic mantle is considered very low (~0.03 wt %) [*McDonough and Sun*, 1995], but the occurrence of K-rich magmatism suggests that the mantle is locally enriched in potassium [*McCulloch et al*., 1983] and includes a discrete phase as a host of potassium in such K-rich portions. Previous experimental studies demonstrated that K phase III appears in K-doped pyrolitic lower mantle material (0.64 wt % K_2O) at 25.5 GPa, coexisting with $MgSiO_3$-rich perovskite, ferropericlase, and $CaSiO_3$-rich perovskite [*Wang and Takahashi*, 2000]. Because the solubility of potassium in typical lower mantle phases is quite limited, *Wang and Takahashi* [2000] argued that the K phase III is present even in normal lower mantle.

[3] K phase III should be identical to the NAL phase [*Miyajima et al*., 1999; *Gasparik et al*., 2000; *Miura et al*., 2000]. NAL is known to form in subducted basaltic crust under uppermost lower mantle conditions [*Miyajima et al*., 2001; *Hirose and Fei*, 2002; *Ricolleau et al*., 2010]. More recent experiments by *Imada et al*. [2011] have shown that the NAL phase only forms below 45 GPa and undergoes transformation into CF at higher pressures on the join $NaAlSiO_4$-$MgAl_2O_4$ [*Ono et al*., 2009]. This is consistent with the disappearance of NAL above ~50 GPa in deeply subducted oceanic crust with mid-oceanic ridge basalt (MORB) composition [*Perrillat et al*., 2006; *Ricolleau et al*., 2008]. Nevertheless, potassium prefers NAL more than CF as demonstrated by high-pressure experiments [*Miyajima et al*., 2001] and by the study of inclusions in superdeep diamonds [*Walter et al*., 2011], indicating that potassium stabilizes NAL relative to CF.

[4] The general formula for NAL is $[M3][M2]_2[M1]_6O_{12}$, where M1, M2, and M3 represent small-, middle-, and large-sized cations, respectively [*Miura et al*., 2000; *Gasparik et al*., 2000]. The structure of NAL has hexagonal symmetry and consists of a double-chain framework of $M1O_6$ octahedra that are connected to each other by sharing the edges. Two differently sized tunnel-like spaces along the *c* axis surrounded by three and six double chains of $M1O_6$ provide the sites for the middle-sized (M2) and relatively large-sized (M3) cations, respectively. Because of the large cation site, NAL can incorporate potassium. *Kojitani et al*. [2011] reported that NAL with $K_{1.00}Mg_{2.00}Al_{4.80}Si_{1.15}O_{12}$ composition contains the maximum amount of potassium (including cation vacancy in the M1 site) and that the M3 site is only occupied by potassium. In this study, we determined the phase relations on the join $Na_{1.00}Mg_{2.00}Al_{4.80}Si_{1.15}O_{12}$-$K_{1.00}Mg_{2.00}Al_{4.80}Si_{1.15}O_{12}$ at 33–144 GPa and 1800–2700 K by combining laser-heated diamond anvil cell techniques and synchrotron X-ray diffraction (XRD). Pressure-volume data of $K_{1.00}Mg_{2.00}Al_{4.80}Si_{1.15}O_{12}$ NAL were also obtained up to 127 GPa and room temperature. The results show that K-rich NAL has a very wide stability *P-T* field that covers the entire lower mantle.

2. Experimental Procedure

[5] We prepared four starting materials from gels with chemical compositions of $Na_{0.75}K_{0.25}Mg_{2.00}Al_{4.80}Si_{1.15}O_{12}$ (Na75K25), $Na_{0.50}K_{0.50}Mg_{2.00}Al_{4.80}Si_{1.15}O_{12}$ (Na50K50), $Na_{0.25}K_{0.75}Mg_{2.00}Al_{4.80}Si_{1.15}O_{12}$ (Na25K75), and $K_{1.00}Mg_{2.00}Al_{4.80}Si_{1.15}O_{12}$ (K100). The composition of the K end-member is taken from *Kojitani et al*. [2011]. The gel was dehydrated by heating to 1273 K for 15 min, and the compositions were confirmed by electron microprobe analysis. The powder sample was pressed into a disc and coated with Au in runs #1–4 and #6–8. In runs #5 and #9–12, the sample was mixed with Au powder at a mass ratio of 10:1. Au was used as a laser absorber and an internal pressure standard. The sample was loaded into

Additional supporting information may be found in the online version of this article.

[1]Department of Earth and Planetary Sciences, Tokyo Institute of Technology, Tokyo, Japan.
[2]Earth-Life Science Institute, Tokyo Institute of Technology, Tokyo, Japan.
[3]Institute for Research on Earth Evolution, Japan Agency for Marine-Earth Science and Technology, Yokosuka, Kanagawa, Japan.
[4]Japan Synchrotron Radiation Research Institute, Sayo, Hyogo, Japan.

Corresponding author: C. Kato, Department of Earth and Planetary Sciences, Tokyo Institute of Technology, 2-12-1 Ookayama, Meguro, Tokyo 152-8551, Japan. (kato.c.ab@m.titech.ac.jp)

0094-8276/13/10.1002/grl.50966

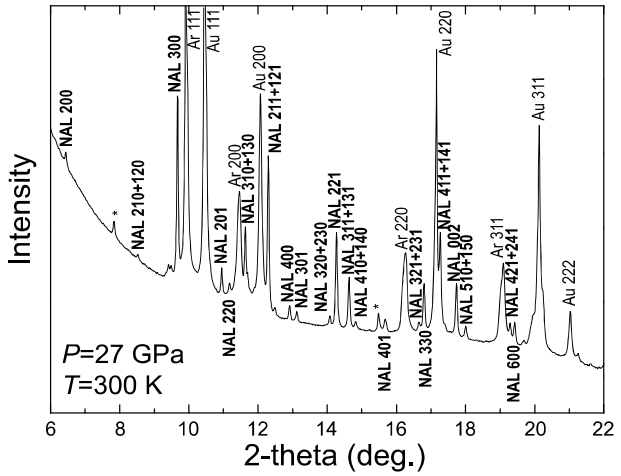

Figure 1. Typical XRD pattern of $K_{1.00}Mg_{2.00}Al_{4.80}Si_{1.15}O_{12}$ (K100) NAL collected after heating at 1900 K and 39 GPa. Asterisks indicate unknown peaks; the same unidentified peaks were previously reported for NAL by *Oguri et al*. [2000], *Shinmei et al*. [2005], and *Imada et al*. [2011]. They possibly indicate the distortion of the crystal structure.

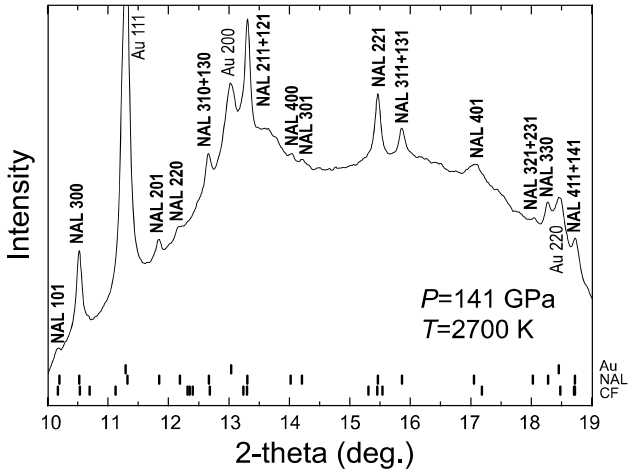

Figure 2. Typical XRD pattern of K100 NAL obtained during heating at 2700 K and 141 GPa. Tick marks represent the calculated major diffraction peaks of Au, NAL, and CF.

the hole of the rhenium gasket together with a pressure medium of Ar, KCl, or a pure starting material unmixed with gold (see Table S1 in the supporting information). The samples were compressed by diamond anvils with a culet size of 300 μm for pressures less than 70 GPa and a culet size of 120–150 μm for higher pressures.

[6] The samples were heated to 1800–2700 K by a multimode yttrium/aluminum/garnet laser or a couple of single-mode Yb fiber lasers at BL10XU, SPring-8. The beam-shaping optics that converts a Gaussian beam to one with a flatter energy distribution was used to reduce the radial temperature gradient. Temperature was measured from both sides by fitting the thermal radiation spectrum to the Planck radiation function using the spectroscopic method. The heating duration was 5–135 min for each run (Table S1). Temperature variations in the 15 μm area from which XRD data were collected were within ±10% [e.g., *Ozawa et al*., 2010].

[7] The angle-dispersive spectra were collected on an imaging plate (Rigaku R-AXIS IV) and a charge-coupled device (Bruker APEX). The wavelength of the monochromatic incident X-ray beam was 0.412–0.415 Å. Sample pressure was calculated from the volume of Au on the basis of the thermal equation of state of *Fei et al*. [2007]. The pressure uncertainty is ±1.4–3.2 GPa and is mainly attributed to the temperature uncertainties.

3. Results

[8] We conducted 12 separate runs and obtained 14 data sets to examine the phase relations on the join $Na_{1.00}Mg_{2.00}Al_{4.80}Si_{1.15}O_{12}$-$K_{1.00}Mg_{2.00}Al_{4.80}Si_{1.15}O_{12}$ (Table S1). While sharp diffraction peaks appeared in less than 5 min at the low-pressure range (Figure 1), crystallization was found to be rather sluggish at greater than 120 GPa. The peaks were weak even after heating to 2700 K at 141 GPa (Figure 2). The XRD patterns of NAL and CF phases are similar to each other, but their characteristic peaks, including those at 10–11° of 2-theta angle, were used for phase identification. In addition, the misfit of peak assignment was much larger when assuming the CF phase instead of the NAL phase in all experiments.

[9] The experiments on the K end-member (K100) demonstrated that NAL was the single phase from 39 GPa and 1900 K to 141 GPa and 2700 K (Figure 3). Earlier multianvil experiments synthesized K100 NAL at 20–25 GPa [*Kojitani et al*., 2011]. These results indicate that K100 NAL is stable in lower mantle *P-T* conditions, although it might melt at the high temperatures of the core-mantle boundary (CMB) region. This strongly contrasts with the fact that K-free (Na100) NAL is stable only below 27 GPa at 1850 K [*Imada et al*., 2011].

[10] Similarly, we observed only NAL in both Na25K75 and Na50K50 compositions at the entire *P-T* range explored in this study. Na50K50 NAL was formed at 144 GPa, with the pressure exceeding that of the CMB. On the other hand, both NAL and CF coexisted at 120 GPa and 2300 K for

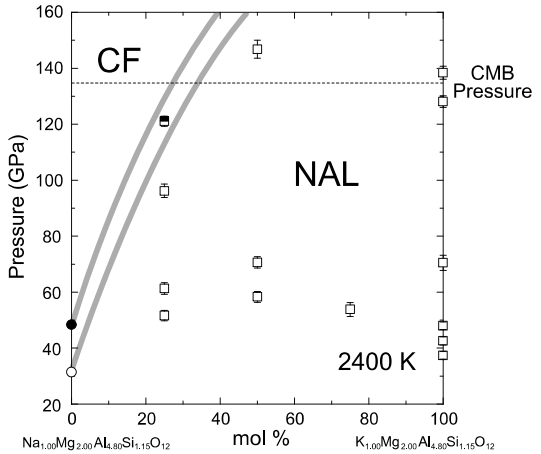

Figure 3. Phase relations on the join $Na_{1.00}Mg_{2.00}Al_{4.80}Si_{1.15}O_{12}$-$K_{1.00}Mg_{2.00}Al_{4.80}Si_{1.15}O_{12}$ at 2400 K. Open squares indicate the formation of single-phase NAL, and the half-filled square demonstrates the coexistence of NAL and CF. Open and closed circles show the CF-in and NAL-out boundaries, respectively, for the Na end-member composition [*Imada et al*., 2011].

the Na75K25 bulk composition (see Figure S1 in the supporting information).

[11] In addition, we have obtained pressure-volume (*P-V*) data for the K end-member (K100) NAL at 300 K between 27 and 127 GPa (Table S2). The volume data were measured right after the synthesis of single-phase NAL in runs #1–5. The lattice constants and the unit-cell volumes were calculated from 14 to 34 diffraction peaks.

4. Stability and Incompressibility of K-rich NAL

[12] The phase relations on the join $Na_{1.00}Mg_{2.00}Al_{4.80}Si_{1.15}O_{12}$-$K_{1.00}Mg_{2.00}Al_{4.80}Si_{1.15}O_{12}$ (Na100-K100) are drawn in Figure 3 considering the earlier experimental results on the join $NaAlSiO_4$-$MgAl_2O_4$ [*Imada et al*., 2011]. *Imada et al*. [2011] reported that Na100 NAL is stable up to 27 GPa, NAL and CF coexist between 27 and 44 GPa, and Na100 and CF form above 44 GPa at 1850 K. In order to draw the composition-pressure phase diagram at 2400 K (Figure 3), the experimental temperatures were corrected by adjusting the pressure on the basis of the *P-T* slope (+0.008 GPa/K) of the NAL-out reaction in MORB [*Perrillat et al*., 2006].

[13] The phase diagram in Figure 3 indicates that NAL forms a continuous solid solution on the join $Na_{1.00}Mg_{2.00}Al_{4.80}Si_{1.15}O_{12}$-$K_{1.00}Mg_{2.00}Al_{4.80}Si_{1.15}O_{12}$ below 32 GPa. More importantly, potassium drastically expands the stability field of NAL. This suggests that the K^+ ion has a strong affinity for the M3 site in the NAL structure not only at 25 GPa [*Kojitani et al*., 2011] but also at deep lower mantle pressures.

[14] We fitted the third-order Birch-Murnaghan equation of state to the *P-V* data of K100 NAL, i.e.,

$$P = \frac{3}{2}K_0\left[\left(\frac{V}{V_0}\right)^{-\frac{7}{3}} - \left(\frac{V}{V_0}\right)^{-\frac{5}{3}}\right]\cdot\left\{1+\frac{3}{4}(K'-4)\left[\left(\frac{V}{V_0}\right)^{-\frac{2}{3}}-1\right]\right\} \quad (1)$$

where V_0, K_0, and K' are unit-cell volume, isothermal bulk modulus, and its pressure derivative, respectively, at ambient conditions. In the fitting procedure, V_0 was fixed at 186.37(1) Å^3, as reported by *Kojitani et al*. [2011]. The fitting yielded $K_0 = 207(2)$ GPa and $K' = 4.1(0)$. The results are shown in Figure S2 and Table S3 in the supporting information and are compared with the results of previous studies on different chemical compositions. We did not observe anomalous compression behavior over the pressure range studied, implying that the 3*s*-4*d* electronic transition of potassium did not take place [*Bukowinski*, 1976].

[15] *Imada et al*. [2012], on the basis of compression experiments, reported that $K_0 = 199(6)$ GPa and $K' = 5.0(6)$ for $Na_{1.2}Mg_{1.8}Al_{4.8}Si_{1.2}O_{12}$ NAL, which is similar in composition to Na100. K' was, however, not well constrained in *Imada et al*. [2012] because the experimental pressure range was limited to 31 GPa. We therefore fitted their *P-V* data with K' fixed at 4.1, same as that obtained for K100 NAL. The results show $K_0 = 207(5)$ GPa for $Na_{1.2}Mg_{1.8}Al_{4.8}Si_{1.2}O_{12}$ NAL, which is identical to that of the K end-member. Note that the refitted parameters reproduce the experimental data of *Imada et al*. [2012] as well as their original parameters. Both *Imada et al*. [2012] and the present study use the Au pressure scale proposed by *Fei et al*. [2007]. Hence, the similar K_0 values imply that the bulk modulus of NAL is not affected by the exchange between Na and K. It may be dominantly controlled by the $(Al,Si)O_6$ double chains that make up the framework of the crystal structure.

5. K-rich NAL in the Lower Mantle

[16] These results indicate that K-rich NAL has a wide stability field, which covers the entire *P-T* conditions of the lower mantle when the molar ratio K:(Na + K) is greater than 0.35 on the join $Na_{1.00}Mg_{2.00}Al_{4.80}Si_{1.15}O_{12}$-$K_{1.00}Mg_{2.00}Al_{4.80}Si_{1.15}O_{12}$ (Figure 3). The multianvil experiments of *Wang and Takahashi* [2000] demonstrated that the NAL phase formed at 25.5 GPa in K-rich (0.64 wt % K_2O) pyrolitic mantle material with a molar ratio K:(Na + K) of ~0.85 (reported as K phase III). K-rich NAL in such natural multicomponent systems has a complex chemical formula, but the main compositional difference with the present study is the high Mg and Si at the expense of Al (see Figure S3 in the supporting information). The recent first-principles calculations by *Mookherjee et al*. [2012] have shown that higher Mg content stabilizes NAL relative to CF, supporting that the NAL phase can be present in the deep lower mantle.

[17] It is known that $CaSiO_3$ perovskite incorporates minor amounts of potassium. Previous experiments by *Hirose et al*. [2005] reported 0.4 wt % K_2O in $CaSiO_3$ perovskite at 60 GPa, whereas *Kesson et al*. [1998] found 1.6–1.8 wt % K_2O at 70–135 GPa. Considering that the lower mantle may include ~5% $CaSiO_3$ perovskite [e.g., *Murakami et al*., 2005], K-rich NAL may appear as a discrete phase when the K_2O content is greater than 0.09 (=1.8 × 0.05) wt %. Note that typical mantle is considered to contain ~0.03 wt % K_2O [*McDonough and Sun*, 1995].

[18] On the other hand, NAL transforms to CF in the middle part of the lower mantle, when the K:(Na + K) value is low (Figure 3). The NAL phase in subducted MORB crust under uppermost lower mantle conditions has a molar ratio K:(Na + K) of 0.16–0.17 [*Hirose and Fei*, 2002]. Such low K:(Na + K) ratio accounts for the disappearance of NAL above ~50 GPa in MORB [*Perrillat et al*., 2006; *Ricolleau et al*., 2010]. In addition, $KAlSi_3O_8$ hollandite II [*Sueda et al*., 2004] can host potassium in subducted continental crust in the uppermost lower mantle [*Ishii et al*., 2012] and is known to be stable at least to 128 GPa [*Hirao et al*., 2008].

6. Summary and Conclusion

[19] Our experiments demonstrate that potassium dramatically stabilizes NAL relative to CF. K-rich NAL appears in the shallow-to-deep lower mantle having a K_2O content higher than 0.09 wt %. The melting phase relations in a K-rich pyrolite composition shows that K-rich NAL (K Phase III) is the last phase to crystallize during cooling and can host potassium at 25.5 GPa [*Wang and Takahashi*, 2000]. If this is also the case at higher pressures, K-rich NAL may crystallize from partial melts in the ultralow-velocity zone. In addition, a large amount of K-rich NAL may have formed in the final solidification stages of a basal magma ocean [*Labrosse et al*., 2007; *Nomura et al*., 2011]. Future studies on the high-temperature elastic property of NAL will elucidate the presence of NAL as a radiogenic heat source above the CMB [*Kawai and Tsuchiya*, 2012; *Dai et al*., 2013].

[20] **Acknowledgments.** We thank M. Mookherjee and an anonymous reviewer for their valuable suggestions. S. Tateno, E. Sugimura, and S. Imada are acknowledged for their help in synchrotron experiments and useful comments.

The in situ XRD experiments were conducted at SPring-8 (proposals 2012A0087 and 2012B0087).

[21] The Editor thanks Mainak Mookherjee and an anonymous reviewer for their assistance in evaluating this paper.

References

Bukowinski, M. S. T. (1976), The effect of pressure on the physics and chemistry of potassium, *Geophys. Res. Lett.*, *3*, 491–494.

Dai, L., Y. Kudo, K. Hirose, M. Murakami, Y. Asahara, H. Ozawa, Y. Ohishi, and N. Hirao (2013), Sound velocities of $Na_{0.4}Mg_{0.6}Al_{1.6}Si_{0.4}O_4$ NAL and CF phases to 73 GPa determined by Brillouin scattering method, *Phys. Chem. Miner.*, *40*, 195–201.

Fei, Y., A. Ricolleau, M. Frank, K. Mibe, G. Shen, and V. Prakapenka (2007), Toward an internally consist pressure scale, *Proc. Natl. Acad. Sci. U. S. A.*, *104*, 9182–9186.

Gasparik, T., A. Tripathi, and J. B. Parise (2000), Structure of a new Al-rich phase, $[K,Na]_{0.9}[Mg,Fe]_2[Mg,Fe,Al,Si]_6O_{12}$, synthesized at 24 GPa, *Am. Mineral.*, *85*, 613–618.

Hirao, N., E. Ohtani, T. Kondo, T. Sakai, and T. Kikegawa (2008), Hollandite II phase in $KAlSi_3O_8$ as a potential host mineral of potassium in the Earth's lower mantle, *Phys. Earth Planet. Inter.*, *166*, 97–104.

Hirose, K., and Y. Fei (2002), Subsolidus and melting phase relations of basaltic composition in the uppermost lower mantle, *Geochim. Cosmochim. Acta*, *66*, 2099–2108.

Hirose, K., N. Takafuji, N. Sata, and Y. Ohishi (2005), Phase transition and density of subducted MORB crust in the lower mantle, *Earth Planet. Sci. Lett.*, *237*, 239–251.

Imada, S., K. Hirose, and Y. Ohishi (2011), Stabilities of NAL and Ca-ferrite-type phases on the join $NaAlSiO_4$-$MgAl_2O_4$ at high pressure, *Phys. Chem. Miner.*, *38*, 557–560.

Imada, S., K. Hirose, T. Komabayashi, T. Suzuki, and Y. Ohishi (2012), Compression of $Na_{0.4}Mg_{0.6}Al_{1.6}Si_{0.4}O_4$ NAL and Ca-ferrite-type phases, *Phys. Chem. Miner.*, *39*, 525–530.

Ishii, T., H. Kojitani, and M. Akaogi (2012), High-pressure phase transitions and subduction behavior of continental crust at pressure-temperature conditions up to the upper part of the lower mantle, *Earth Planet. Sci. Lett.*, *357–358*, 31–41.

Kawai, K., and T. Tsuchiya (2012), Phase stability and elastic properties of the NAL and CF phases in the $NaMg_2Al_5SiO_{12}$ system from first principles, *Am. Mineral.*, *97*, 305–314.

Kesson, S. E., J. D. Fitz Gerald, and J. M. Shelley (1998), Mineralogy and dynamics of a pyrolite lower mantle, *Nature*, *393*, 252–255.

Kojitani, H., T. Iwabuchi, M. Kobayashi, H. Miura, and M. Akaogi (2011), Structure refinement of high-pressure hexagonal aluminous phases $K_{1.00}Mg_{2.00}Al_{4.80}Si_{1.15}O_{12}$ and $Na_{1.04}Mg_{1.88}Al_{4.64}Si_{1.32}O_{12}$, *Am. Mineral.*, *96*, 1248–1253.

Labrosse, S., J. W. Hernlund, and N. Coltice (2007), A crystallizing dense magma ocean at the base of the Earth's mantle, *Nature*, *450*, 866–869.

Lee, K. K. M., G. Steinle-Neumann, and S. Akber-Knutson (2009), Ab initio predictions of potassium partitioning between Fe and Al-bearing $MgSiO_3$ perovskite and post-perovskite, *Phys. Earth Planet. Inter.*, *174*, 247–253.

McCulloch, M. T., A. L. Jaques, D. R. Nelson, and J. D. Lewis (1983), Nd and Sr isotopes in kimberlites and lamproites from Western Australia: an enriched mantle origin, *Nature*, *302*, 400–403.

McDonough, W. F., and S. S. Sun (1995), The composition of the Earth, *Chem. Geol.*, *120*, 223–253.

Miura, H., Y. Hamada, T. Suzuki, M. Akaogi, N. Miyajima, and K. Fujino (2000), Crystal structure of $CaMg_2Al_6O_{12}$, a new Al-rich high pressure form, *Am. Mineral.*, *85*, 1799–1803.

Miyajima, N., K. Fujino, N. Funamori, T. Kondo, and T. Yagi (1999), Garnet-perovskite transformation under conditions of the Earth's lower mantle: an analytical transmission electron microscopy study, *Phys. Earth Planet. Inter.*, *116*, 117–131.

Miyajima, N., T. Yagi, K. Hirose, T. Kondo, K. Fujino, and H. Miura (2001), Potential host phase of aluminum and potassium in the Earth's lower mantle, *Am. Mineral.*, *86*, 740–746.

Mookherjee, M., B. B. Karki, L. Stixrude, C. Lithgow-Bertelloni (2012), Energetics, equation of state, and elasticity of NAL phase: Potential host for alkali and aluminum in the lower mantle, *Geophys. Res. Lett.*, *39*, L19306, doi:10.1029/2012GL053682.

Murakami, M., K. Hirose, N. Sata, and Y. Ohishi (2005), Post-perovskite phase transition and mineral chemistry in the pyrolitic lowermost mantle, *Geophys. Res. Lett.*, *32*, L03304, doi:10.1029/2004GL021956.

Nomura, R., H. Ozawa, S. Tateno, K. Hirose, J. Hernlund, S. Muto, H. Ishii, and N. Hiraoka (2011), Spin crossover and iron-rich silicate melt in the Earth's deep mantle, *Nature*, *473*, 199–202.

Oguri, K., N. Funamori, T. Uchida, N. Miyajima, T. Yagi, and K. Fujino (2000), Post-garnet transition in a natural pyrope: a multi-anvil study based on in situ X-ray diffraction and transmission electron microscopy, *Phys. Earth Planet. Inter.*, *122*, 175–186.

Ono, A., M. Akaogi, H. Kojitani, K. Yamashita, and M. Kobayashi (2009), High-pressure phase relations and thermodynamic properties of hexagonal aluminous phase and calcium-ferrite phase in the systems $NaAlSiO_4$-$MgAl_2O_4$ and $CaAl_2O_4$-$MgAl_2O_4$, *Phys. Earth Planet. Inter.*, *174*, 39–49.

Ozawa, H., K. Hirose, S. Tateno, N. Sata, and Y. Ohishi (2010), Phase transition boundary between B1 and B8 structures of FeO up to 210 GPa, *Phys. Earth Planet. Inter.*, *179*, 157–163.

Perrillat, J. P., A. Ricolleau, I. Daniel, G. Fiquet, M. Mezouar, N. Guignot, and H. Cardon (2006), Phase transformations of subducted basaltic crust in the upmost lower mantle, *Phys. Earth Planet. Inter.*, *157*, 139–149.

Ricolleau, A., G. Fiquet, A. Addad, N. Menguy, C. Vanni, J. P. Perrillat, I. Daniel, H. Cardon, and N. Guignot (2008), Analytical transmission electron microscopy study of a natural MORB sample assemblage transformed at high pressure and high temperature, *Am. Mineral.*, *93*, 144–153.

Ricolleau, A., J. P. Perrillat, G. Fiquet, I. Daniel, J. Matas, A. Addad, N. Menguy, H. Cardon, M. Mezouar, and N. Guignot (2010), Phase relations and equation of state of a natural MORB: Implications for the density profile of subducted oceanic crust in the Earth's lower mantle, *J. Geophys. Res.*, *115*, B08202, doi:10.1029/2009JB006709.

Shinmei, T., T. Sanehira, D. Yamazaki, T. Inoue, T. Irifune, K. Funakoshi, and A. Nozawa (2005), High-temperature and high-pressure equation of state for the hexagonal phase in the system $NaAlSiO_4$-$MgAl_2O_4$, *Phys. Chem. Miner.*, *32*, 594–602.

Sueda, Y., T. Irifune, N. Nishiyama, R. P. Rapp, T. Ferroir, T. Onozawa, T. Yagi, S. Merkel, N. Miyajima, and K. Funakoshi (2004), A new high-pressure form of $KAlSi_3O_8$ under lower mantle conditions, *Geophys. Res. Lett.*, *31*, L23612, doi:10.1029/2004GL021156.

Walter, M. J., S. C. Kohn, D. Araujo, G. P. Bulanova, C. B. Smith, E. Gaillou, J. Wang, A. Steele, and S. B. Shirey (2011), Deep mantle cycling of oceanic crust: Evidence from diamonds and their mineral inclusions, *Science*, *334*, 54–57.

Wang, W., and E. Takahashi (2000), Subsolidus and melting experiments of K-doped peridotite KLB-1 to 27 GPa: Its geophysical and geochemical implications, *J. Geophys. Res.*, *105*, 2855–2868, doi:10.1029/1999JB900366.